

Ultraviolet fluorescence excitation and emission spectroscopy of marine algae and bacteria

Stephan Determann^{a,1}, Jörg M. Lobbes^{a,b,2}, Rainer Reuter^{a,*}, Jürgen Rullkötter^b

^a Carl von Ossietzky Universität Oldenburg, Fachbereich Physik, P.O. Box 2503, D-26 111 Oldenburg, Germany

^b Carl von Ossietzky Universität Oldenburg, Institut für Chemie und Biologie des Meeres (ICBM), P.O. Box 2503, D-26 111 Oldenburg, Germany

Received 21 May 1997; accepted 10 February 1998

Abstract

Ultraviolet (UV) excitation and emission spectra of cultures of marine bacteria and phytoplankton were investigated. The intensity of the emission band at 340 nm wavelength ($\lambda_{\text{ex}} = 230$ nm) is compared with cell number and protein content, and specific efficiencies are derived. Another weak emission band at 305 nm is found with most phytoplankton species. The same fluorescence signatures are observed with protein fragments and proteins of known composition and are caused by their tryptophan and tyrosine content. The UV fluorescence of marine particles is related to these aromatic amino acids bound to proteins. © 1998 Elsevier Science B.V. All rights reserved.

Keywords: ultraviolet fluorescence; tryptophan; tyrosine; bacteria; phytoplankton

1. Introduction

Fluorescence has been a tool for the study of organic matter in seawater for a long time. Measurements of phytoplankton chlorophyll *a* at 685 nm wavelength are well known (see for example the review article of Krause and Weis, 1991). Also, the fluorescence of chromophoric constituents of dissolved organic matter (DOM, gelbstoff) at blue–

green wavelengths has been the subject of many investigations since its first observation by Kalle (1963).

Lately, fluorescence of seawater in the 270 to 360 nm range has met increasing interest. First reported by Traganza (1969), these signals were attributed to proteins or aromatic amino acids and their metabolites (Ewald et al., 1986; Coble et al., 1990; Mopper and Schultz, 1993; De Souza Sierra et al., 1994). Determann et al. (1994) denoted specific fluorescence emission bands with maxima at 280 and 325 nm as tyrosine-like and tryptophan-like fluorescence. The emission signature resembles the fluorescence of these free aromatic amino acids (Tatischeff and Klein, 1976), but with shifts to shorter wavelengths due to their binding in proteins (Wolfbeis, 1985; Lakowicz, 1986).

* Corresponding author.

¹ Present address: Universität Bremen, Fachbereich Geowissenschaften, D-28359 Bremen, Germany.

² Present address: Alfred-Wegener-Institut für Polar- und Meeresforschung, Columbusstraße, D-27568 Bremerhaven, Germany.

Ultraviolet fluorescence of biomolecules, like proteins and nucleic acids is well known in biology and medicine. Recently, tryptophan-like fluorescence of bacterial cells has been successfully used in biotechnology, for example, to control fermentation in bioreactors (Li and Humphrey, 1990) and to detect bacterial biofilms (Angell et al., 1993). Also, laboratory cultures of marine bacteria (Daltiero et al., 1986), algae (Baek et al., 1988; Petersen, 1989) and coral extracts (Matthews et al., 1996) have been found to give rise to tryptophan-like fluorescence.

Few efforts have been made to identify in more detail the substances that produce UV fluorescence in seawater. Signals from DOM in the visible range were of higher interest in most investigations reported in the literature, and water samples were usually filtered before analysis. As with the blue-green gelbstoff fluorescence, UV protein-like fluorescence has then been attributed to dissolved organic molecules (Mopper and Schultz, 1993; De Souza Sierra et al., 1994; Coble, 1996). However, glass fiber or nylon filters with pore sizes in the 0.5 to 1 μm range cannot retain small particles such as bacteria. Our investigations made with unfiltered samples from the Atlantic Ocean (Determann et al., 1994) have led us to the assumption that an essential part of the tryptophan and tyrosine-like fluorescence arises from aromatic amino acids bound to particles. Measurements in cultures of bacteria (Determann et al., 1996; Determann, 1996) further supported this hypothesis.

In this paper, we report results of detailed fluorescence excitation and emission analyses of marine algae and bacteria. The purpose of this study is to present quantitative spectra that are specific to these marine particles. Their fluorescence is compared with signals from metabolites of aromatic amino acids and from proteins of known composition. The types of fluorophores are classified, and relations are given which connect fluorescence intensity to bacterial and algal biomass.

2. Methods

2.1. Bacteria

Cultures of sixteen bacteria species isolated from marine and littoral samples (Table 1) were cultivated

in Zobell medium (Zobell, 1946) at about 30°C. To simulate the growth and decay of bacteria under near-natural conditions, two cultures were held in seawater enriched with algal exudates. The two batch cultures were kept at room temperature in amber bottles without shaking, and their development was analyzed in time-series measurements over periods of three months.

The background fluorescence from dissolved molecules of the medium was so strong that a water Raman signal was hardly detectable with $\lambda_{\text{ex}} = 230$ nm. Also, the high absorption coefficient of the medium gave rise to absorption losses especially in the UV and blue which would have severely distorted the fluorescence spectra (internal quenching). Therefore, nineteen bacteria cultures (Table 1) were cleaned before a fluorometric measurement. This was done by centrifuging the samples at $15,000 \times g$ at room temperature for at least 15 min until bacterial pellets had been formed. The pellets were resuspended in a sterile 0.85% NaCl solution prepared with MilliQ water and analytical grade NaCl. Each sample was centrifuged four times, with resuspension in NaCl solution between each centrifugation. To check the linearity of fluorescence data, the cultures were analyzed in six to eight runs at different particle concentrations (Fig. 1); again, the 0.85% NaCl solution was used to dilute the samples. The correlation coefficient of signal versus particle concentration is $r^2 > 0.99$ for a given bacterium species.

Fluorescence emission from organic impurities of the NaCl solution was separately checked in each individual measurement and mostly found to be below 5% of the fluorescence from particles. To derive fluorescence spectra specific to particles, the small background signal from the NaCl solution was calculated by extrapolation of measurements at different dilution steps to zero concentration of bacteria. To derive spectra which are specific to bacteria alone, this signal was subtracted from the sample spectra of one dilution step.

Cell numbers and protein content of one dilution step per sample were analyzed parallel to fluorescence measurements. The total bacterial number (TBN) was obtained by counting with an epifluorescence microscope (Hobbie et al., 1977). For this, a small sample volume was filtered through a black 0.2 μm Nuclepore filter. The bacteria on the filter

Table 1

Fluorescence efficiency of bacteria. Relation of $\lambda_{\text{ex}} = 230 \text{ nm} / \lambda_{\text{em}} = 330 \pm 5 \text{ nm}$ fluorescence (Flu) to the total bacterial number (TBN) and protein concentration (Pro). Spectral ex/em resolution: 5/8 nm. Fluorescence intensities are given in Raman units (RU)/nm. Relative errors given by the standard deviation Δ are derived from the regression of data measured at different particle concentrations, from the uncertainty in the water Raman normalization and the TBN and protein measurements

Culture name (origin)	Symbol in Fig. 1	Flu/TBN [(10 ⁻³ RU/nm) / (10 ⁸ cells/ml)]	Δ (Flu/TBN) [%]	Flu/Pro [(10 ⁻³ RU/nm) / ($\mu\text{g/ml}$)]	Δ (Flu/Pro) [%]
<i>Planococcus</i>	○	5.6	11.6	138.8	9.2
<i>Serratia marioruba</i>	+	47.7	11.7	326.1	9.3
<i>S. marioruba</i>	plus inside square	5.6	12.5	91.4	10.3
<i>Aeromonas sobria</i>	—	23.4	12.0	257.9	9.6
<i>A. sobria</i>	▲	22.2	11.6	321.4	9.2
<i>A. marii</i>	*	23.6	14.9	184.0	13.0
<i>A. marii</i>	◆	34.3	11.2	332.3	8.6
<i>Klebsiella oxytoca</i>	■	11.6	12.7	121.5	10.6
<i>Morganella morganii</i>	plus inside diamond	35.3	11.3	302.1	8.7
92/104 (Baltic Sea)	□	9.2	12.8	78.3	10.6
92/159 (Baltic Sea)	plus inside triangle	18.0	12.2	146.7	9.9
alt 147 (Persian Gulf)	⊕	25.0	11.3	188.5	8.8
alt 878 (eastern Atlantic)	x	31.4	11.5	214.2	9.0
alt 878 (eastern Atlantic)	∇	37.5	11.3	259.9	8.7
alt 1570 (eastern Atlantic)	x inside rectangle	4.3	12.0	96.6	9.7
alt 1725 (eastern Atlantic)	◇	52.1	11.3	230.4	8.7
alt 1902 (Azores)	⊗	69.3	15.2	118.5	13.4
alt 1902 (Azores)	▼	13.8	11.2	320.7	8.6
alt 1782 (Baltic Sea)		25.2	11.2	238.6	8.7
alt 1782 (Baltic Sea)	△	11.5	11.3	251.6	8.8
alt 1918 (Azores)	●	12.9	12.5	102.4	10.2
alt 2800 (Atlantic)	○	9.8	11.4	67.0	8.9
Average		24 ± 16		200 ± 88	

surface were colored with acridine orange for 3 min. Cell numbers were then calculated as the average of 40 individual microscopic countings. The relative error of TBN data is about 10%. During time-series measurements, particle sizes were also determined using a New Porton grid (May, 1965). The cell volume and the cell carbon content were computed according to formulas given by Bratback (1985) and Simon and Azam (1989), respectively. No correction has been made for possible cell shrinkage caused by the sample preparation.

The protein content was measured with the method of Bradford (1976). Three millilitre samples of the cultures were centrifuged at 15,000 × g at room temperature for 20 min. The pellets were resuspended in 100 μl 1 N NaOH and heated at 100°C for 10 min to bring the cellular protein into solution. After adding 700 μl purified water and 200 μl

Bradford solution, the absorption spectrum was measured photometrically. With the time-series measurements, 15 ml sample volumes were centrifuged at 13,000 × g for 20 min, and the pellets were resuspended in 2 ml purified water and treated with ultrasonication for 2 min. Finally, 500 μl Bradford solution were added. A calibration of photometric readings versus protein content was done with solutions of bovine serum albumin (BSA) with known protein concentrations. To check the results for outliers, the protein analyses were made with duplicate or triplicate samples. The relative error of these data is 7%.

2.2. Algae

Fourteen marine algae species from four different algae classes (Table 2) were cultivated in F/2

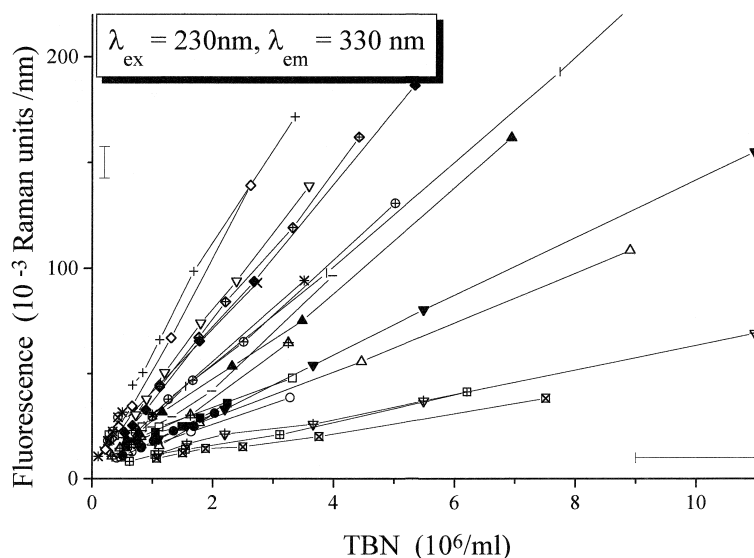


Fig. 1. Fluorescence of bacteria cultures as a function of the total bacteria number (TBN). Excitation/emission wavelengths are $\lambda_{\text{ex}} = 230$ nm/ $\lambda_{\text{em}} = 330 \pm 5$ nm. Fluorescence intensities are given in Raman units/nm, see Section 2.4. Each line describes the signals from an individual culture at different particle concentrations, with symbols given in Table 1. The highest value of the culture alt 1782 (symbol \downarrow) with $397 \cdot 10^{-3}$ Raman units/nm at $15.5 \cdot 10^6$ particles per millilitre is not shown. Error bars denote the relative error of fluorescence and TBN measurements. The data have not been corrected for the weak background signals from the NaCl solution.

medium (Guillard and Ryther, 1962). The samples were kept at a temperature of 12°C and a light intensity of $70\text{--}100 \mu\text{E}/(\text{m}^2\text{s})$ for 24 h per day. Because of the risk of cell breaking during filtration or centrifugation, the sample cleaning procedure used with the bacteria was not applied. Instead, a fraction of each culture was carefully filtered with Whatman GF/F filters at a small negative pressure difference. The filtrate was then used to dilute the original sample in four steps. In this way, four samples with the same culture medium and hence, concentration of dissolved fluorescent matter but different particle concentrations were prepared. Fluorescence measurements were done with the filtrate and with samples at each dilution step, from which algae-specific spectra were derived (Fig. 2). In this way, the data could also be checked for possible errors, such as nonlinearities due to self-absorption of light, sedimentation of particles in the fluorimeter cuvette, or changes of the filtrate characteristics. As with the bacteria, the correlation coefficient of background corrected signal intensity versus particle concentration is $r^2 > 0.99$.

Particle numbers were determined with the method of Utermöhl (1958). After adding 4% Formol solution, 10 ml of sample were put into a sedimentation cell, and allowed to settle in the dark at 4°C for several hours. The particles were then counted with a microscope. The estimated error is 10%.

Protein was determined according to Bradford (1976). For this, 100 or 200 ml of the sample were filtered with Whatman GF/F filters at a small pressure difference. To bring the cell content into solution, the frozen filter and a few millilitres of purified water were treated with ultrasonics at 0°C . Particulate material was then removed by centrifuging 1.5 ml of the suspension at $16,300 \times g$. A $150 \mu\text{l}$ aliquot of 1 N NaOH and 3 ml Bradford solution were added to $300 \mu\text{l}$ of the particle-free solution and photometrically analyzed. Calibration of the photometer was done with BSA as a known standard. The relative error of protein measurements is 7%.

The tryptophan content of algae cultures was measured by HPLC. The algae were filtered with Whatman GF/F filters and immediately frozen at -25°C . Alkaline hydrolysis of the particulate matter

Table 2

Fluorescence efficiency of phytoplankton. Relation of $\lambda_{\text{ex}} = 230 \text{ nm} / \lambda_{\text{em}} = 330 \pm 15 \text{ nm}$ fluorescence (Flu) to cell numbers (CN) and protein (Pro) and tryptophan (Trp) concentrations, and their relative error given by the standard deviation Δ . Spectral ex/em resolution: 7/7 nm. Fluorescence intensities are given in Raman units (RU)/nm. Relative errors given by the standard deviation Δ are derived from the linear regression of data measured at different particle concentrations, from the uncertainty in the water Raman normalization and the cell number, protein and tryptophan measurements

Phytoplankton class	Phytoplankton species	Symbol in Fig. 2	Flu/CN [(10 ⁻³ RU/nm) / (10 ³ cells/ml)]	$\Delta(\text{Flu}/\text{CN})$ [%]	Flu/Pro [(10 ⁻³ RU/nm) / ($\mu\text{g}/\text{ml}$)]	$\Delta(\text{Flu}/\text{Pro})$ [%]	Flu/Trp [(10 ⁻³ RU/nm) / ($\mu\text{mol}/\text{ml}$)]	$\Delta(\text{Flu}/\text{Trp})$ [%]
Bacillariophyceae	<i>Ditylum brightwelli</i>	*	58.31	27.2	113.4	26.2		
	<i>Nitzschia sp.</i>	●	0.83	22.6			1908	21.4
	<i>Skeletonema costatum</i>	□	45.41	26.8	208.6	25.9		
Chlorophyceae	<i>Dunaliella tertiolecta</i>	▲	8.99	23.3	119.2	22.2		
	<i>D. tertiolecta</i>	—	2.69	25.3	31.0	24.3	558	24.3
Prymnesiophyceae	<i>Chrysochromulina sp.</i>	⊕	2.33	25.6				
	<i>Chrysochromulina sp.</i>	■	1.98	25.4	40.1	24.4	2005	24.4
	<i>Phaeocystis sp.</i>	+	1.47	25.4	67.6	24.4	902	24.4
	<i>Phaeocystis globosa</i>		1.51	26.7	19.5	25.7	895	25.7
	<i>P. globosa</i>	◆	0.23	23.4	113.7	22.3		
	<i>Prymnesium parvum</i>	not shown			24.5	20.7	3429	20.7
Haptophyceae	<i>Isochrysis sp.</i>	x	3.60	26.6	90.1	25.6	1469	25.6
	<i>Isochrysis sp.</i>	▼	2.19	23.1	132.0	21.9		
Rhodophyceae	<i>Rhodomonas sp.</i>	not shown			115.8	24.6	1158	24.6
Average			11 ± 19		90 ± 53		(1.54 ± .86) · 10 ³	

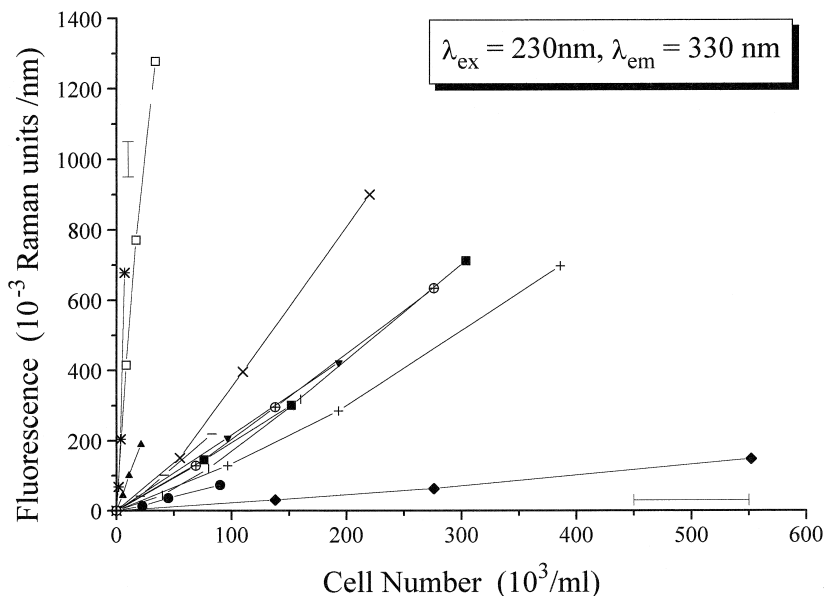


Fig. 2. Fluorescence of algae cultures as a function of the particle concentration, with symbols given in Table 2. $\lambda_{\text{ex}} = 230 \text{ nm} / \lambda_{\text{em}} = 330 \pm 15 \text{ nm}$. Straylight and fluorescence background from the culture medium are removed as described in Section 2.2.

including the filter was done with 2 ml 5 N NaOH solution at 110°C for 24 h. To prevent the amino acids from oxidizing, 100 μl 1% ascorbic acid solution were added (Robertson et al., 1987). The hydrolysed samples were set to pH 9.5 using hydrochloric acid. Amino acids were derivatized with *o*-phthalaldehyde (OPA) and 2-mercaptoethanol. They were separated and detected with a Beckman model Gold HPLC analyser equipped with a diode array absorption detector and an RP18 column. For gradient elution, three mobile phases were used: A) acetonitrile and 12.5 mM Na_2HPO_4 buffer 10:90, B) acetonitrile and 12.5 mM Na_2HPO_4 buffer 50:50, and C) acetonitrile, 12.5 mM Na_2HPO_4 buffer and methanol 45:45:10. The buffer was adjusted to pH 7.2. The flow rate was set to 1.6 ml/min. Start conditions were 100:0:0, going via 76:24:0 to 0:0:100 in 69 min. (Schneider and Földi, 1986).

Calibration of the HPLC analyser was done with amino acid solutions of various known concentrations. The recovery rate of free dissolved tryptophan after hydrolysis was about 120%. No attempts have been made to account for modifications in concentration of amino acids due to hydrolysis with correction

factors derived from these calibration measurements. The relative error is estimated to 7%.

2.3. Proteins and protein fragments, aromatic amino acids and metabolites

The standard proteins, BSA and human serum albumin (HSA), and the protein fragments, Polistes–Mastoparan (PM) and insulin receptor kinase substrate (IRKS) dissolved in purified water, were fluorometrically analysed in native form and after denaturation with 10 mmol (BSA, HSA) and 20 mmol (PM, IRKS) sodium dodecyl sulphate (SDS). Protein structure (Peters, 1985; Hansen, 1990) and aromatic amino acid content of these standards are known (Table 3). The proteins were analyzed at room temperature in a 12.5 mmol Na_2HPO_4 buffer at pH 7.0, the protein fragments in a 10.0 mmol Na_2HPO_4 buffer at pH 7.0.

Fluorescence spectra from metabolites of tryptophan were taken at room temperature and at concentrations of 0.24 $\mu\text{mol/l}$ dissolved in 12.5 mmol/l Na_2HPO_4 buffer solution at pH 7.2, metabolites of tyrosine and phenylalanine at concentrations of 2.9

Table 3

Number of aromatic amino acids per protein of the standard proteins bovine serum albumin (BSA)^a and human serum albumin (HSA)^a, and the protein fragments Polistes–Mastoparan (PM)^b and insulin receptor kinase substrate (IRKS)^b

	BSA	HSA	PM	IRKS
Tryptophan	2	1	1	0
Tyrosine	19	18	0	1
Phenyl alanine	27	31	0	0
Total number of amino acids	582	585	13	13

^aSigma, Deisenhofen, Germany.

^bBachem, Heidelberg, Germany.

PM: H-Val-Asp-Trp-Lys-Ile-Gly-Gln-His-Ile-Leu-Ser-Val-Leu-NH₂.

IRKS: H-Arg-Arg-Leu-Ile-Glu-Asp-Ala-Glu-Tyr-Ala-Ala-Arg-Gly-OH.

$\mu\text{mol/l}$ dissolved in 10 mmol/l Na₂HPO₄ buffer solution at pH 7.0. This is equivalent to the concentration of these aromatic amino acids in a 5 mg/l BSA solution.

2.4. Fluorescence

Fluorescence spectra were measured with a Perkin–Elmer Model LS-50 Luminescence Spectrometer. Cuvettes were cleaned with a 20% HNO₃ solution and heated at 280°C for 4 h. Spectral calibration of the instrument was done as described in Determann et al. (1994). Fluorescence intensities are standardized to the integrated water Raman scatter band for the given excitation wavelength and denoted as Raman units. Conversion factors of the Raman unit to intensity scales derived from the fluorescence of quinine sulfate are given in Determann et al. (1996). For example, one Raman unit/nm corresponds to 310 ± 15 fluorescence units (flu) at $\lambda_{\text{ex}} = 325 \text{ nm}/\lambda_{\text{em}} = 450 \text{ nm}$ (Chen and Bada, 1992), and to 2.1 ± 0.1 quinine sulfate units (QSU) at $\lambda_{\text{ex}} = 350 \text{ nm}/\lambda_{\text{em}} = 450 \text{ nm}$ (Mopper and Schultz, 1993).

Spectra from algal cultures are often obscured by stray light from particles that are insufficiently blocked by the excitation and emission monochromators of the spectrometer. This false light did not occur with the bacteria samples due to their much smaller cell size, and hence lower scattering efficiency. To correct the spectra from algae for such

erroneous signals, a false light spectrum was measured with a suspension of BaSO₄ which is an almost ideal scattering and non-fluorescent material.

To further derive fluorescence data as specific as possible for the fluorescence of algae, the measured emission and excitation spectra with $\lambda_{\text{ex}} = 230 \text{ nm}$ and $\lambda_{\text{em}} = 340 \text{ nm}$, respectively, were processed as follows. In a first step, spectra from the filtrates were subtracted from the total spectra of the algae suspensions. Hence, fluorescence from the culture medium cancels out, the result is a composite of fluorescence and stray light which originates from particles only. Second, spectra were corrected for stray light. This was done by subtracting the BaSO₄ spectrum after its multiplication with a constant factor so that the emission spectra derived in this way yield a near-to-zero signal at $\lambda_{\text{em}} = 270\text{--}280 \text{ nm}$, and the excitation spectra at $\lambda_{\text{ex}} = 310\text{--}315 \text{ nm}$. The rationale of this step is the low fluorescence emission and excitation from algae at these wavelengths, so that the spectra are assumed to be dominated by stray light there.

3. Results

3.1. Bacteria

Excitation and emission spectra of 22 bacteria species (Table 1) are shown in Fig. 3. To compare their band shapes, the curves are normalized to identical maximum intensities. Fluorescence contributions from the culture medium—in this case a low fluorescence NaCl solution—have been eliminated from the data, as described above. This procedure also eliminates water Raman scattering. Therefore, the figure displays signals which arise from bacteria exclusively.

The emission spectra at 230 nm excitation, Fig. 3a, consist of a single fluorescence band with a maximum at about 325 nm. Signal intensities are virtually zero at wavelengths below 280 nm. This holds also in the entire visible range, not shown in Fig. 3, where signals are close to the detection limit. Excitation spectra are characterized by two absorption bands with maxima at about 225 and 280 nm (Fig. 3b). These bands appear to belong to the same fluorophore since the linear correlation coefficient of

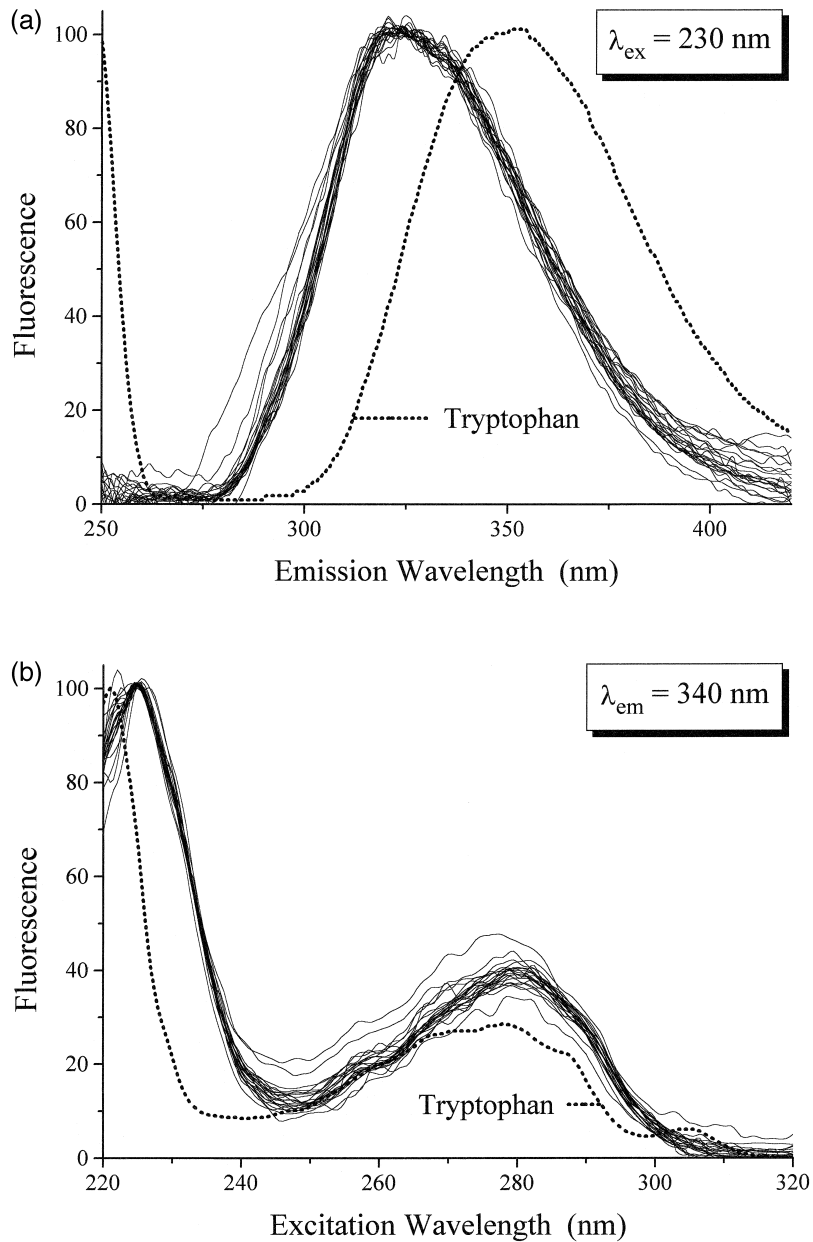


Fig. 3. Fluorescence spectra of bacteria given in Table 1, compared to free dissolved tryptophan (dotted line). (a) emission spectra with $\lambda_{\text{ex}} = 230 \text{ nm}$, normalized to identical average intensities in the 320 to 330 nm range. Ex/em bandwidth 5/8 nm, scan speed 150 nm/min. Peak position: 325 nm with 10 nm variance. The full width half maximum (fwhm) is 60 nm with 10 nm variance. The slope at 250–260 nm of the tryptophan spectrum is the trailing edge of water Raman scattering which has its maximum at 250 nm. (b) excitation spectra with $\lambda_{\text{em}} = 340 \text{ nm}$, normalized to same intensity in the 224 to 226 nm range. Ex/em bandwidth 5/10 nm, scan speed 200 nm/min. Peak position of the first band is at 225 nm with 5 nm variance; fwhm is 25 nm with 15 nm variance. Peak position of the second band is at 280 nm with 15 nm variance; fwhm is 35 nm with 15 nm variance. The small peak at 305 nm is water Raman scattering. The tyrosine spectrum is not given because of low efficiency at 340 nm emission wavelength.

the 340 nm emission with $\lambda_{\text{ex}} = 225$ nm and 280 nm is $r = 0.99$. The constant shape of these spectral bands is obvious from the figures; they reflect a single spectral signature. An average excitation/emission matrix of all investigated species has been derived, which describes the excitation bands centered at 225 and 280 nm in detail (Fig. 4).

Spectra of free tryptophan dissolved in pure water are shown by the dotted lines in Fig. 3a and b for comparison. The spectra of free tryptophan and bacteria have virtually the same band shape. However, the emission spectra of bacteria have a blue shift of about 20 to 25 nm, the excitation spectra a red shift of 5 nm when compared to free dissolved tryptophan.

To investigate the specific fluorescence efficiencies of bacterial cultures in detail, fluorescence data were normalized to TBN (Table 1). It is evident from Fig. 1 that such relations are strongly species-dependent. The efficiency of different cultures typically varies by an order of magnitude. However, the actual state of a given culture plays a comparably strong role as well. This is seen from the results of duplicate measurements made on several cultures (Table 1). On an average, 10^6 cells/ml give rise to a signal

of about $24 \cdot 10^{-3}$ Raman units/nm at $\lambda_{\text{ex}} = 230$ nm/ $\lambda_{\text{em}} = 330$ nm.

Protein-specific fluorescence efficiencies are of interest since the bacterial biomass expressed as protein content compensates for differences in particle sizes of the various species. The average fluorescence at $\lambda_{\text{ex}} = 230$ nm/ $\lambda_{\text{em}} = 330$ nm normalized to protein is 0.20 Raman units/nm per mg/l protein concentration. The variability in this parameter between cultures is only a factor of three (Table 1), much lower than the efficiency normalized to TBN, as expected.

However, the establishment of an accurate relation of fluorescence efficiency versus bacterial biomass is also hampered by methodological uncertainties in the biomass measurement. This is evident in the data of two time-series measurements with natural batch cultures consisting of mixed populations. A plot of fluorescence versus protein yields fluorescence to protein ratios which vary by a factor of four to five (Fig. 5a). Culture conditions of both time-series measurements were nutrient limited since the growth of the bacteria reached a stationary phase at the tenth day of the experiment. Nutrient limitations are mostly connected with a comparatively

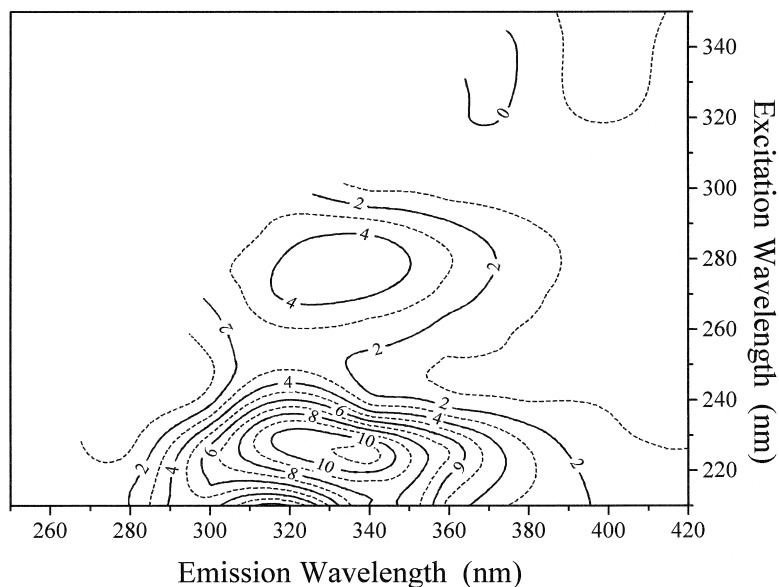


Fig. 4. Average fluorescence excitation/emission matrix of bacteria. The individual data were normalized to 10 at $\lambda_{\text{ex}} = 225$ nm/ $\lambda_{\text{em}} = 340$ nm, before the average of all species was calculated.

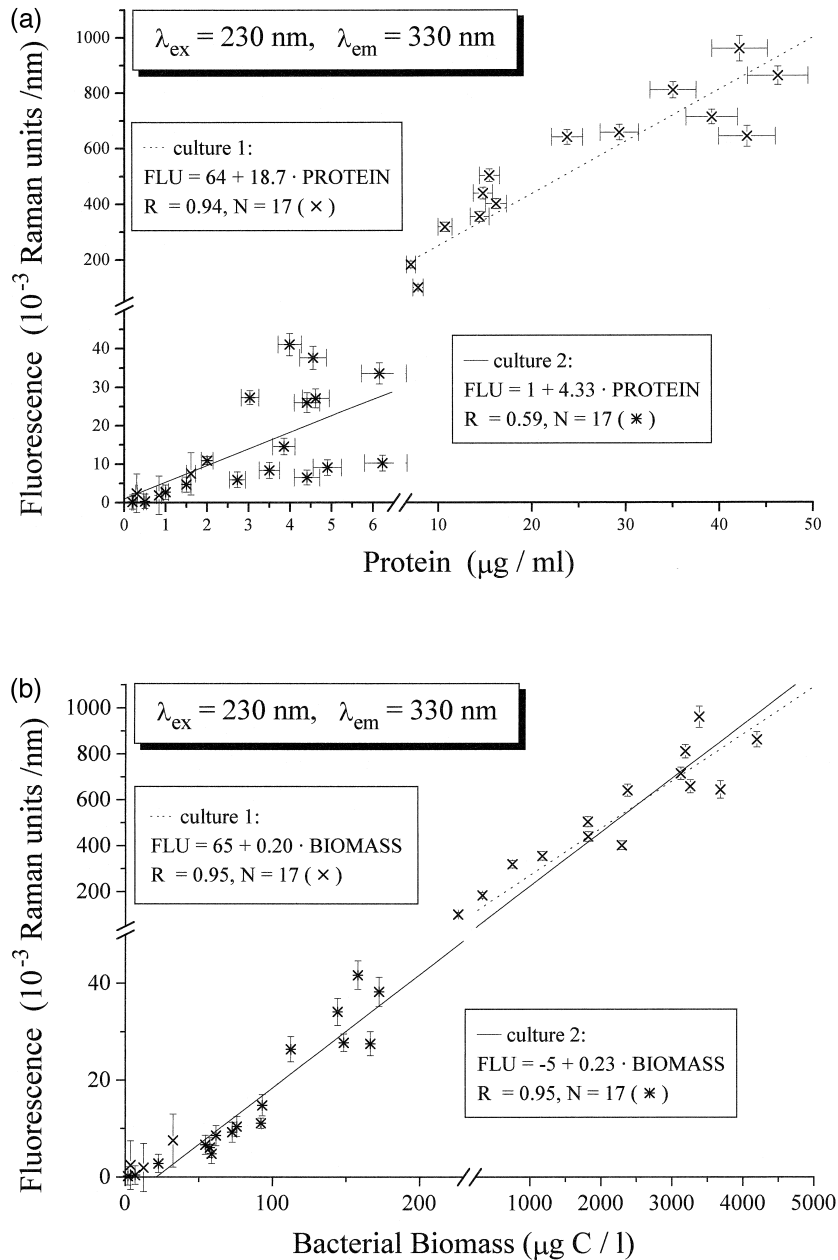


Fig. 5. (a) Fluorescence of two bacteria cultures in 100 days time-series experiments versus protein concentration according to the method of Bradford (1976). $\lambda_{\text{ex}} = 230 \text{ nm}/\lambda_{\text{em}} = 330 \pm 5 \text{ nm}$. A linear regression yields different slopes for culture 1 (dotted line) and culture 2 (full line) as indicated, with FLU in Raman units/nm and protein in $\mu\text{g}/\text{ml}$. (b) Fluorescence plotted versus bacterial organic carbon determined according to Simon and Azam (1989) as described in the text. Linear regression of culture 1 (dotted line) and culture 2 (full line), with biomass in $\mu\text{g} \text{ C}/\text{l}$. The regression of culture 2 is extrapolated to the data points of culture 1, to show the near-identical behaviour of both cultures.

Table 4

Comparison of fluorescence efficiencies from two 100 day time-series measurements with bacteria cultures, and the average data from bacteria cultures given in Table 1

	Flu/TBN [(10 ⁻³ RU/nm) / (10 ⁶ cells/ml)]	Flu/Protein [(10 ⁻³ RU/nm) / (μg/ml)]	Flu/C _{org} [(10 ⁻³ RU/nm) / (μg/l)]
Culture 1	8.9 ± 3.0	20.9 ± 8.4	280 ± 110
Culture 2	3.9 ± 1.6	4.7 ± 2.8	160 ± 50
Average from Table 1	24 ± 16	200 ± 88	not det.

higher cellular protein content (Simon and Azam, 1989). The same parameters of the cultures given in Table 1 take on much higher values (Table 4).

In these time-series measurements, the cell carbon content was additionally calculated using the empirical relation (Simon and Azam, 1989)

$$\text{cell carbon content}/\text{fg}/\text{cell} = 1.048 \cdot 88.6$$

$$(\text{average cell volume}/\mu\text{m}^3)^{-0.59}.$$

By multiplication with TBN, the data were converted to the total bacterial organic carbon content C_{org} of the sample. A plot of fluorescence versus bacterial C_{org} derived in this way leads to a much better correlation of the data from each culture, and to a reasonable covariance of both time-series measurements, Fig. 5b. With C_{org} derived in this way as a parameter of the bacterial biomass, the fluorescence efficiency of the cultures differs by less than a factor of 2. It is obvious from these results that fluorescence shows a much higher covariance to the total C_{org} content derived from cell volume and particle number, than to the protein content.

3.2. Algae

Emission spectra from algal cultures were corrected for fluorescence contributions from the medium and for monochromator stray light, as described in Section 2.2 and 2.4, to derive algae-specific signals. However, the data might include signals from bacteria in unknown quantities since bacteria attached to algae could not be separated by filtration. Emission spectra (Fig. 6a) are markedly more variable than those from bacteria in terms of both the positions of the maxima and the bandwidths. The average peak position of the emission spectra is at 340 nm, 15 nm longer than the maximum position

found with bacteria. The linear correlation coefficient of the 340 nm emission with $\lambda_{\text{ex}} = 225$ nm and 280 nm is $r = 0.81$, lower than the correlation found with the bacteria.

A closer view of the data shows that the emission spectra can be grouped into two categories. The spectra from *Nitzschia* spp. and *Prymnesium parvuum* have small bandwidths and shorter peak emission wavelengths (Fig. 6a). They consist of a single emission band, with a band shape similar to tryptophan and a blue shift of 25 nm, as has been observed with bacteria (Fig. 3a). The second larger group of spectra is characterized by peak positions and bandwidths mentioned above. Part of the variability at the leading edge is due to another emission band in the 300 nm range. A comparison with the emission of free dissolved tyrosine shows that this peak might be from tyrosine, since their position and widths are virtually identical. None of the spectra from bacteria has shown the same tyrosine-like contribution at their leading edge, and this holds also for the *Nitzschia* spp. and *P. parvuum* spectra. The main emission band is again similar to the fluorescence of free dissolved tryptophan.

Excitation spectra (Fig. 6b) are again similar to, but more variable than, those of bacteria. In particular, the 280 nm band intensity is often very weak. In some cases, this leads to an almost constant signal from 240 to 290 nm, and a specific band at 280 nm cannot be identified. With a few exceptions, the peak of the main absorption band in the 220 to 230 nm range does not show the same red shift as with bacteria. However, its apparent variability might in part be due to an imperfect stray light correction of the spectra.

Fluorescence intensities normalized to phytoplankton cell numbers are a function of the species,

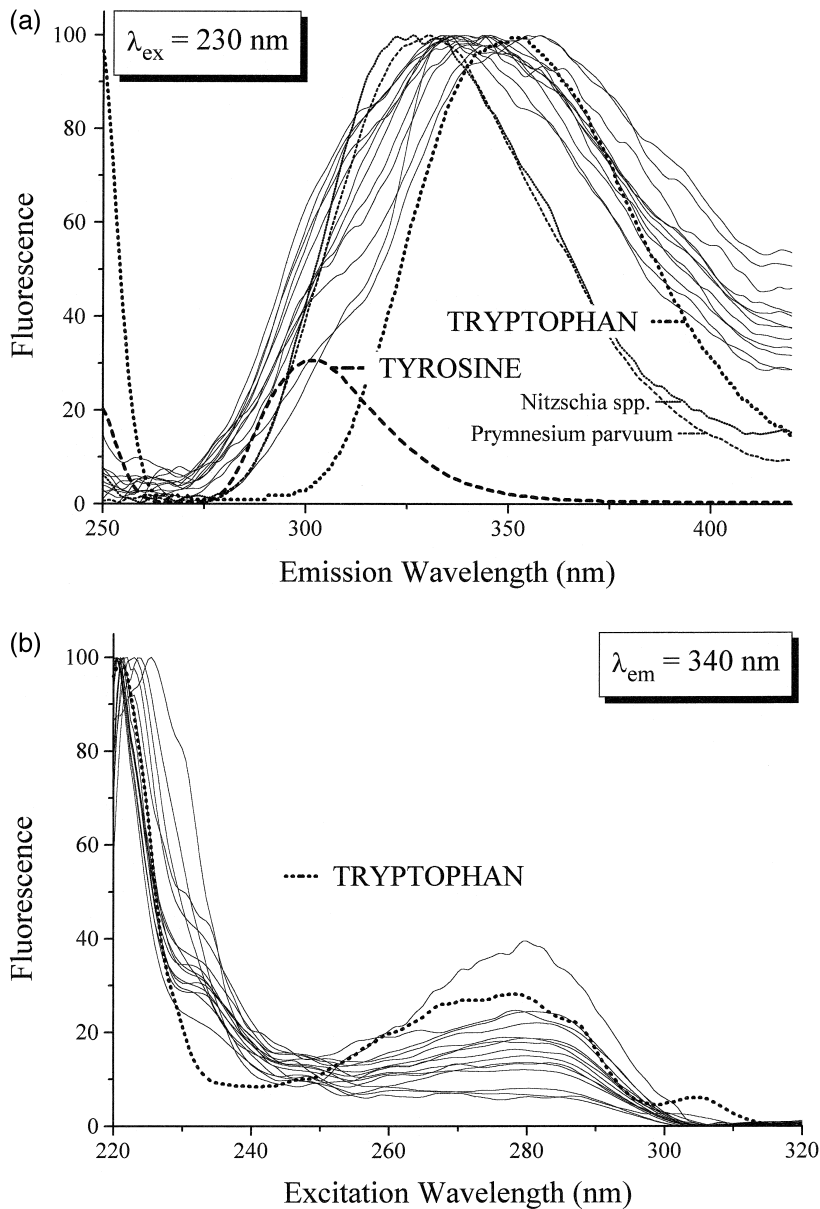


Fig. 6. Fluorescence spectra of algae species given in Table 2, compared to free dissolved tryptophan and tyrosine (dotted lines, arbitrary intensity scales). (a) emission spectra with $\lambda_{ex} = 230$ nm, normalized to identical maximum intensity. Ex/em bandwidth 7/7 nm, scan speed 400 nm/min, noise reduction by a 10 nm moving average. Peak position: 340 nm with 20 nm variance. The full width half maximum (fwhm) is 80 nm with 35 nm variance. The weak structures at 420 nm are considered artifacts from insufficiently corrected monochromator stray light. The slopes at 250–260 nm of the tryptophan and tyrosine spectra are the trailing edge of water Raman scattering. (b) excitation spectra with $\lambda_{em} = 340$ nm, normalized to identical maximum intensities. Ex/em bandwidth 7/7 nm, scan speed 400 nm/min, noise reduction by 5 nm moving average. Peak position of the first band is at 225 nm with 5 nm variance; fwhm is 25 nm with 5 nm variance. Peak position of the second band is at 280 nm with 15 nm variance; fwhm is 45 nm. The small peak at 305 nm in the tryptophan spectrum is water Raman scattering. The tyrosine spectrum is not given because of low efficiency at 340 nm emission wavelength.

and also dependent on the physiological status, i.e., the age, illumination and light history of a given culture (Table 2). On an average, 10^3 cells/ml yield a signal intensity of $10 \cdot 10^{-3}$ Raman units/nm at $\lambda_{\text{ex}} = 230 \text{ nm} / \lambda_{\text{em}} = 330 \text{ nm}$. More stable relations are obtained if intensities are related to the protein concentration. Then, the efficiency typically is $90 \cdot 10^{-3}$ Raman units/nm per $\mu\text{g}/\text{ml}$ of protein, which is about two times lower than the average efficiency of the analyzed bacteria cultures. Fluorescence normalized to the tryptophan concentration measured with HPLC (Section 2.2) yielded an efficiency of about $1.6 \cdot 10^{-3}$ Raman units/nm per $\mu\text{mol}/\text{l}$ tryptophan. The variability between species is a factor of four, about the same as in the data normalized to protein. The fluorescence efficiency of free tryptophan dissolved in water is $0.83 \cdot 10^{-3}$ Raman units/nm per $\mu\text{g}/\text{l}$, or $170 \cdot 10^{-3}$ Raman units/nm per $\mu\text{mol}/\text{l}$ tryptophan (Determann et al., 1994). Hence, the efficiency of tryptophan bound to phytoplankton protein is about two orders of magnitude lower than the efficiency of free dissolved molecules.

4. Discussion

The very constant tryptophan-like fluorescence signature of marine bacteria species is evident from the data given in Section 3. Compared to free tryptophan dissolved in water, the spectral position of the emission band shows a blue shift. The same shift is typical of this amino acid when bound in proteins (Wolfbeis, 1985). The fluorescence signature of algae is similar to that of bacteria, but with a more variable spectral position of the excitation and emission bands. On its leading edge, the tryptophan-like emission of algae is often overlapped by a tyrosine-like signal.

Only proteins containing the aromatic amino acids tryptophan, tyrosine or phenylalanine exhibit native fluorescence (Wolfbeis, 1985). However, other types of aromatic molecules might also contribute to these intracellular signals, for example, amino acid metabolites or other fluorophores. Fluorescence of aromatic molecules depends on their ligand structure. For example, tyrosine has a much higher efficiency than phenylalanine, although, they differ only by an OH group as an additional ligand of the aromatic

side chain of the tyrosine molecule. The OH group leads to a higher dipole moment of tyrosine in the excited state, and hence, a better fluorescence efficiency (Wehry and Rogers, 1966; Wehry, 1973). Similarly, small differences in the ligand structure are typical of many metabolic derivatives of aromatic amino acids, and these differences can strongly alter the spectroscopic behavior.

Therefore, some metabolites of tryptophan and of tyrosine/phenylalanine were investigated as possible candidates of fluorescent molecules in cells. These molecules can fluoresce with an efficiency comparable to the aromatic amino acids (Wolfbeis, 1985), however, experimental conditions given in the literature are mostly not representative for particles in seawater. The goal of our measurements was to analyze the fluorescence intensity and bandshape of these natural products in neutral solutions, assuming a similar spectral characteristic when bound to cells.

Emission spectra of tryptophan and its metabolites—indole, skatole and hydroxyanthranilic acid—are given in Fig. 7a. Substance concentrations are $0.24 \mu\text{mol}/\text{l}$. This would be equivalent to a protein concentration of $5 \mu\text{g}/\text{ml}$, assuming the same specific tryptophan concentration as in BSA.

The efficiency and bandshape of indole and skatole are similar to that of free dissolved tryptophan, but with small shifts of about 15 nm of their maxima to shorter and higher wavelengths, respectively. These molecules can contribute to the tryptophan-like fluorescence if present in cells in quantities that are comparable to tryptophan. The blue fluorescence of hydroxyanthranilic acid is not found in bacteria and phytoplankton. The same argument holds with kynurenine, not shown here. Oxadipic acid was also investigated, but the fluorescence efficiency is weak with excitation below 300 nm.

The phenylalanine/tyrosine metabolites—dopamine, noradrenaline, adrenalin and catechol—were analyzed at concentrations of $2.9 \mu\text{mol}/\text{l}$ and the spectra compared with that of tyrosine (Fig. 7b). Again, these concentrations would correspond to the tyrosine content in $5 \mu\text{g}/\text{ml}$ protein, assuming the same composition as in BSA. These metabolites show a slight red shift of about 15 nm in their emission maxima, and the fluorescence efficiency is lower than for tyrosine. The absence of tyrosine-like signals in the case of bacteria, and the generally low

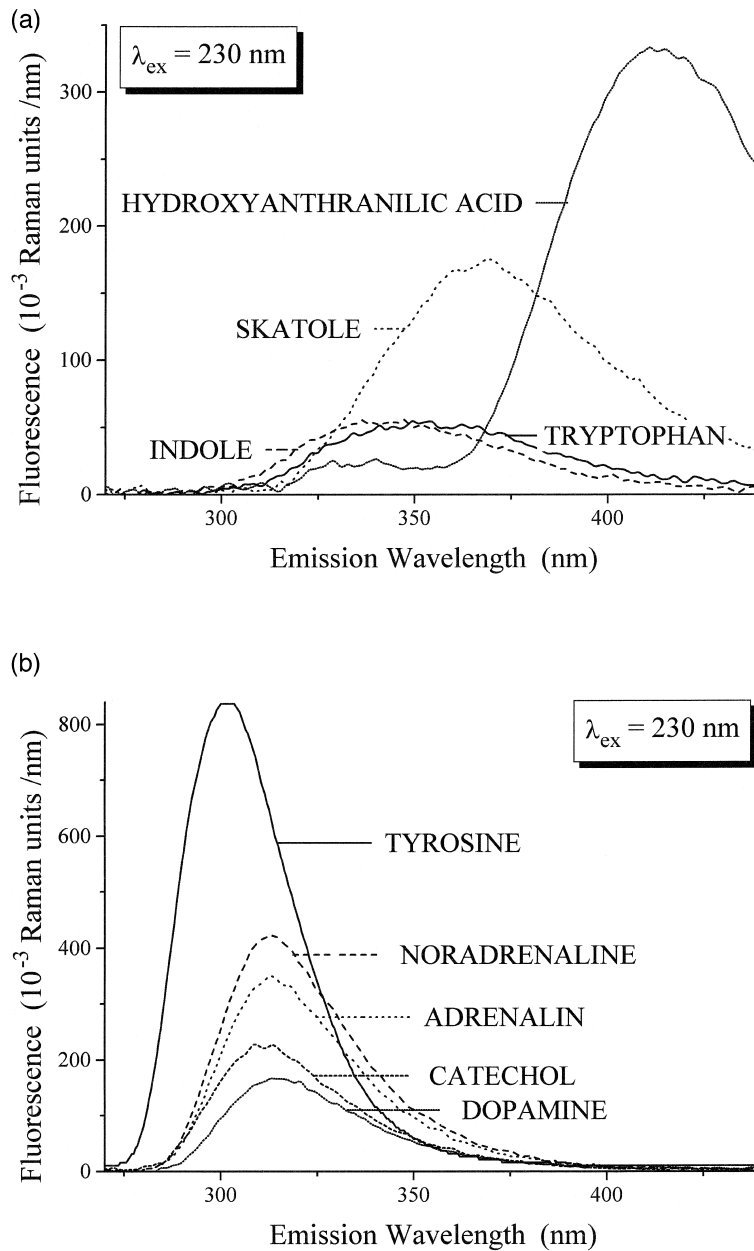


Fig. 7. Emission spectra of tryptophan, tyrosine and their metabolites. $\lambda_{\text{ex}} = 230 \text{ nm}$, ex/em bandwidth 7/7 nm, scan speed 200 nm/min. Signal background from buffer and water is subtracted to show the substance-specific emission. (a) tryptophan and its metabolites indole, skatole and hydroxyanthranilic acid. Substance concentrations are $0.24 \mu\text{mol/l}$. (b) tyrosine and its metabolites noradrenaline, adrenalin, catechol, and dopamine. Substance concentrations are $2.9 \mu\text{mol/l}$.

tyrosine-like fluorescence of phytoplankton leads to the conclusion that these metabolites of tyrosine do not play a role as fluorophores in cells.

Other tryptophan metabolites such as tryptamine, serotonin and dimethyl tryptamine, not investigated here, emit at about 340–360 nm with an efficiency

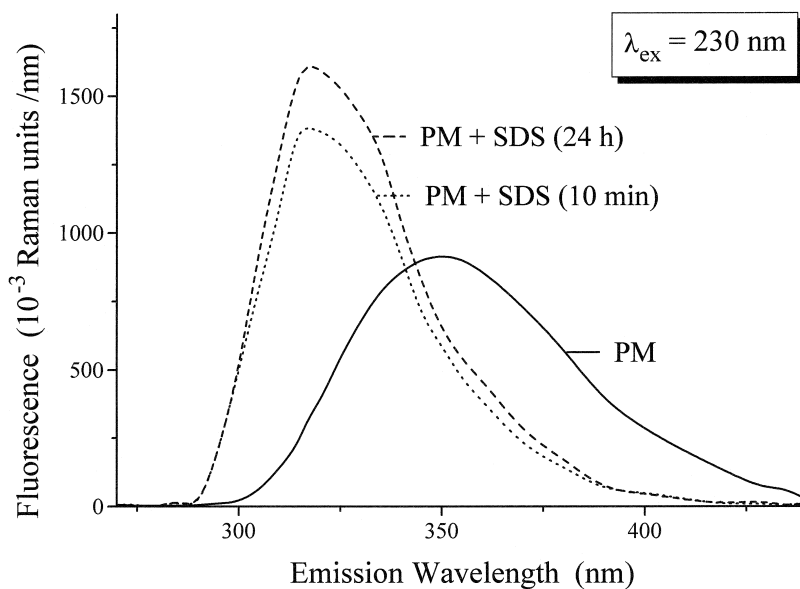


Fig. 8. Emission spectra of the native protein fragment Polistes–Mastoparan, and 10 min and 24 h after denaturation with SDS. Concentration 2.5 mg/l. Instrumental settings as in Fig. 7.

comparable to tryptophan when excited at 270 nm wavelength, as reviewed by Wolfbeis (1985). In view of the comparatively small metabolite concentration in cells, a contribution from such molecules to the cell-specific fluorescence emission is unlikely.

The fluorescence of aromatic amino acids in proteins depends on the specific sequence of amino acids and the presence of quenching molecular groups in the vicinity of the aromatic units. This results in a variable fluorescence efficiency of aromatic amino

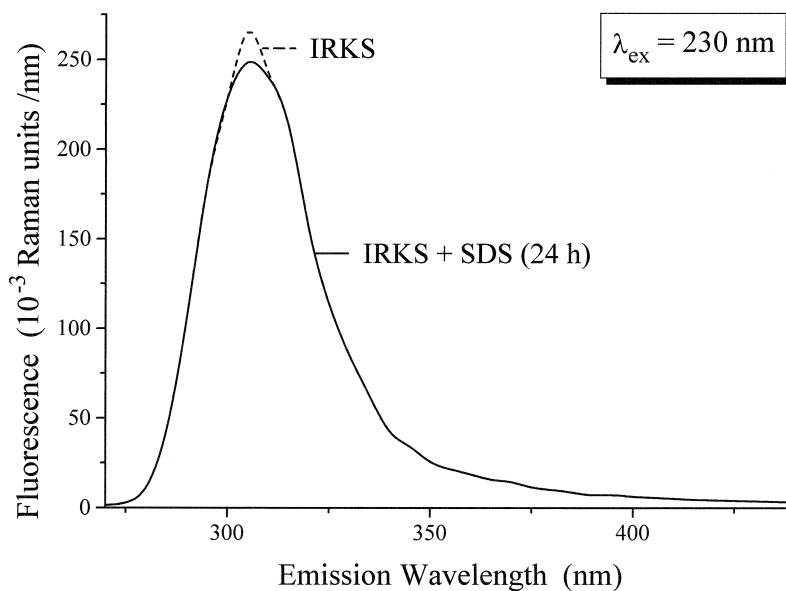


Fig. 9. Emission spectra of the native protein fragment IRKS and 24 h after denaturation with SDS. Concentration = 2.5 mg/l. Instrumental settings as in Fig. 7.

acids bound into different proteins. Energy transfer from phenylalanine to tyrosine and from tyrosine to tryptophan further reduces the fluorescence efficiency of phenylalanine and tyrosine (Stryer, 1978; Daltiero et al., 1986). Also, tryptophan-to-tryptophan energy transfer associated with non-radiative losses has been observed (Toulme et al., 1984).

The influence of the amino acid sequence can be investigated by denaturation of the proteins (Reynolds and Tanford, 1970). Denaturation converts the native protein into a structure with a uniform micro-environment and lower polarity, which neutralizes quenching effects. After denaturation, a linear relation can be expected for the fluorescence signal versus the aromatic amino acid concentration (Shelton and Rogers, 1971).

To further examine these effects, protein fragments with known amino acid sequences were analyzed in native form and after denaturation with SDS (Section 2.3). The protein fragment PM contains one tryptophan and the fragment IRKS contains one tyrosine unit in their amino acid sequences (Table 3). Their fluorescence signatures (Figs. 8 and 9) are virtually the same as the emission of the free aromatic amino acids dissolved in water. Hence, quenching effects, if ever present, do not markedly affect the spectral position of the emission bands (Table 5). Denaturation with SDS has a strong impact on the PM spectrum; its emission is enhanced and shifted to shorter wavelengths (Fig. 8). The signal in the IRKS spectrum remains almost unchanged upon denaturation (Fig. 9).

This agrees with other observations where the fluorescence of tyrosine in protein was found to be independent of the polarity of its environment (Dargan et al., 1983). Tryptophan shows a blue shift of 15 to 50 nm when bound into a less polar micro-environment (Eisinger and Navon, 1969; Galla

et al., 1985). However, emission maxima at around 345 nm of denatured proteins were also reported, as reviewed by Wolfbeis (1985). In our measurement, the blue shift of tryptophan in denatured PM is 33 nm. SDS itself does not act as a quencher since the efficiency of the protein fragments increases after denaturation or remains unchanged.

A comparison with the data of free dissolved tryptophan and tyrosine is interesting. The efficiencies of the free amino acids in their emission bands, (Fig. 7a,b) while considering the different molar concentrations there, are almost the same. When bound to the protein fragments, tryptophan fluoresces three to five times more strongly than tyrosine. This agrees with findings of Wolfbeis (1985) that protein-bound tyrosine fluorescence, in the absence of tryptophan, is only about 10% that of free tyrosine.

The proteins HSA and BSA were utilized to investigate the spectral effects of such processes. These standard proteins have a known composition and include about the same total number of amino acids. The tryptophan content of BSA is twice as high as that of HSA (Table 3). The tryptophan-like fluorescence of the native proteins in the 340 nm region reflects this ratio well. The tyrosine content is approximately the same, and this holds also with the weaker tyrosine-like fluorescence at 300 nm (Fig. 10). These signatures are virtually identical with the emission of phytoplankton cells (Fig. 6a). Apparently, the tryptophan and tyrosine content of many phytoplankton species is close to that of BSA.

Denaturation of the proteins with SDS results in an apparent loss of the 340 nm emission band, and both spectra are dominated by a fluorescence band centered at 304 nm (Fig. 10). In principle, their spectral positions and bandshapes could be explained by tyrosine bound to proteins (Fig. 9), or by trypto-

Table 5

Spectral data of standard proteins and protein fragments in their original form and denatured with SDS. Substances were dissolved in 10 mmol/l NaH₂PO₄ buffer solution and analyzed at room temperature. The data of tryptophan and tyrosine are given for comparison; their fluorescence is not altered in the presence of SDS. $\lambda_{\text{ex}} = 230$ nm, ex/em resolution 5/8 nm

	BSA/BSA + SDS	HSA/HSA + SDS	PM/·PM + SDS	IRKS/IRKS + SDS	Trp	Tyr
Peak pos. [nm]	336/304	337/304	350/317	305/305	355	302
fwhm [nm]	70/49	83/40	64/42	33/31	65	34

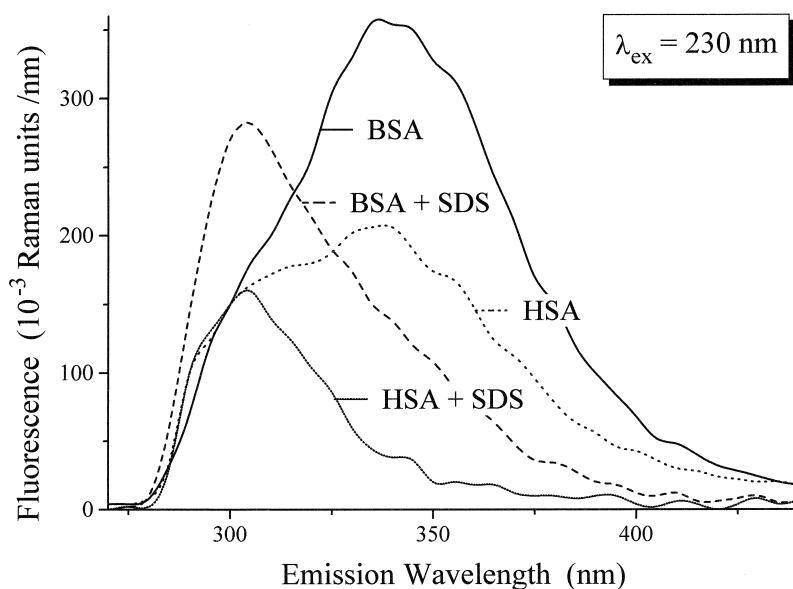


Fig. 10. Emission spectra of the standard proteins BSA and HSA in native form, and after denaturation with SDS. Concentration = 5.0 mg/l. Instrumental settings as in Fig. 7.

phan in denatured proteins (Fig. 8). However, the intensity ratio of BSA-to-HSA fluorescence is again close to a factor of two, as is the tryptophan content ratio. It is therefore concluded that tryptophan is the dominating source of protein fluorescence, in the 340 nm range in native form and in the 305 nm range in denatured proteins. Tyrosine emitting at 305 nm with native and denatured proteins plays a comparatively smaller role.

5. Conclusions

Fluorescence of proteins and protein fragments with known content of tryptophan and tyrosine have been compared with other aromatic compounds of living cells such as metabolites of these aromatic amino acids. It has been shown that the fluorescence signature of native proteins is in good agreement with observations on living marine bacterial and phytoplankton cells. Emission of cells in the 340 nm region is explained by intracellular tryptophan. Phytoplankton can exhibit an additional 305 nm emission band from tyrosine bound to proteins, which is not observed with bacteria.

The bandshapes of metabolites of aromatic amino acids differ from those of tryptophan and tyrosine in free and bound forms. The concentration of these fluorophores in cells would be too small to explain their UV fluorescence emission.

Our investigations have shown that bacteria fluoresce only in the 300 to 370 nm region when excited at wavelengths lower than 300 nm. They do not produce significant signals at higher excitation/emission wavelengths. Some phytoplankton species show low fluorescence signals also at wavelengths above 400 nm, which seems to result mainly from the red shift of the tryptophan emission band compared with that of bacteria. We therefore conclude that, except for the presence of large plankton numbers, seawater fluorescence in the blue and green originates from dissolved organic matter such as gelbstoff alone. On the other hand, our results do not answer the question of whether the emission bands in seawater at 300 to 350 nm originate exclusively from organic particulates. Free dissolved molecules such as exudates from living cells with tryptophan or tyrosine derivatives as aromatic side chains probably also contribute to the UV fluorescence of seawater.

The fluorescence efficiency of bacterial cells, normalized to their protein content, is species-dependent

and varies by a factor of three. The results from time-series measurements made with mixed populations show a stable covariance of fluorescence efficiency to the intracellular carbon content, better than to protein. With 230 nm excitation, the peak intensity of the emission band is on the order of 0.2 Raman units/nm per mg/l protein concentration. At the same wavelength, the standard protein HSA with a 0.1% tryptophan content yields the same peak intensity per 5 mg/l (Fig. 9). Hence, the average protein-specific fluorescence of protein in bacterial cells is about five times higher than the efficiency of this standard protein dissolved in water.

On an average, 10^6 bacterial cells per millilitre give rise to a signal of about $24 \cdot 10^{-3}$ Raman units/nm at $\lambda_{\text{ex}} = 230 \text{ nm}/\lambda_{\text{em}} = 330 \text{ nm}$. These are typical bacterial numbers in the near-surface layer of the ocean and about an order of magnitude higher than at greater depths. Vertical profiles of UV fluorescence in the open ocean well reflect signal intensities in that range. Fig. 11 shows the covariance of fluorescence and TBN measured at two stations in the eastern Atlantic Ocean. The results

from laboratory cultures of natural populations (Fig. 5) are given in the same figure for comparison. Signals from these cultures and from the vertical profiles follow approximately the same trend; differences are in the range of variability which are typical for these parameters, as discussed above.

On an average, the peak fluorescence efficiency of phytoplankton is 0.09 Raman units/nm of protein, two times lower than the efficiency of bacterial protein. The very similar tryptophan emission band at 340 nm of bacteria and phytoplankton does not allow their classification with fluorescence in the UV. The tyrosine band at 305 nm seems to be a characteristic feature of most phytoplankton species. However, it is weak compared with the tryptophan signal and difficult to detect because of the overlap of both emission bands.

About 10^3 phytoplankton cells/ml give rise to the same fluorescence as 10^6 bacterial cells at $\lambda_{\text{ex}} = 230 \text{ nm}/\lambda_{\text{em}} = 330 \text{ nm}$. Such numbers are often found near the sea surface. Hence, UV fluorescence is generally a combined effect from algae and bacteria in the photic zone.

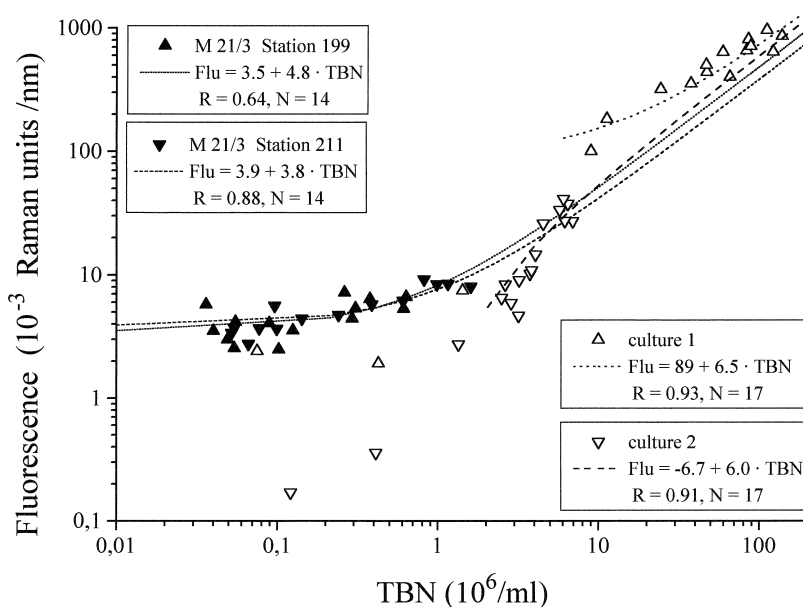


Fig. 11. Plot of fluorescence of unfiltered and untreated water samples versus TBN at two stations in the eastern Atlantic Ocean, R/V Meteor cruise M21/3. Station 199 at position $33^{\circ}56' \text{ N } 21^{\circ}50' \text{ W}$ on May 11th, 1992; station 211 at position $47^{\circ}35' \text{ N } 19^{\circ}30' \text{ E}$ on May 20th, 1992. Data measured from water samples taken with Niskin bottles between surface and 5300 and 4600 m depth, respectively. $\lambda_{\text{ex}} = 230 \text{ nm}/\lambda_{\text{em}} = 330 \pm 5 \text{ nm}$, ex/em bandwidth 7/7 nm. Data of specific bacterial fluorescence from the laboratory cultures 1 and 2 (Fig. 5) are shown for comparison.

Acknowledgements

We are grateful to Dr. H.-J. Rick and Dr. E. Rhiel at the ICBM, Universität Oldenburg, for making available the algae cultures, and to Mrs. M. Mehrens and Dr. S. Ulrich at the Institut für Meereskunde, Kiel, for making available the bacteria cultures, Prof. K. Lochte from the Institut für Ostseeforschung, Warnemünde, and Mrs. C. Grahl from the Alfred-Wegener-Institut für Polar- und Meeresforschung, Bremerhaven, for counting the bacteria in the time-series measurement and discussion of the results. Dr. Ulrich made also available the TBN data from M21/3 stations 199 and 211 shown in Fig. 11. The careful reviews of Dr. Paula G. Coble from the University of South Florida and from two anonymous reviewers were considerably helpful in improving the manuscript. Part of this work was supported by the Federal Minister of Research and Technology, Bonn, in the frame of the JGOFS North Atlantic project.

References

- Angell, P., Arrage, A.A., Mittelman, M.W., White, D.C., 1993. On line, non-destructive biomass determination of bacterial biofilms by fluorometry. *J. Microbiol. Meth.* 18, 317–327.
- Bradford, M.M., 1976. A rapid and sensitive method for the quantification of microgram quantities of protein utilizing the principle of protein-dye binding. *Anal. Biochem.* 72, 248–254.
- Bratback, G., 1985. Bacterial biovolume and biomass estimations. *Appl. Environ. Microbiol.* 49, 1488–1493.
- Baek, M., Nelson, W.H., Hargraves, P.E., Tanguay, J.F., Suib, S.L., 1988. The steady-state and decay characteristics of protein tryptophan fluorescence from algae. *Appl. Spectroscopy* 42, 1405–1412.
- Chen, R.F., Bada, J.L., 1992. The fluorescence of dissolved organic matter in seawater. *Mar. Chem.* 37, 191–221.
- Coble, P., Green, S.A., Blough, N.V., Gagosian, R.B., 1990. Characterization of dissolved organic matter in the Black Sea by fluorescence spectroscopy. *Nature* 348, 432–435.
- Coble, P.G., 1996. Characterization of marine and terrestrial DOM in seawater using excitation–emission matrix spectroscopy. *Mar. Chem.* 51, 325–346.
- Daltiero, R.A., Nelson, W.H., Britt, D., Sperry, J., Psaras, D., Tanguay, J.F., Suib, S.L., 1986. Steady-state and decay characteristics of protein tryptophan fluorescence from bacteria. *Appl. Spectroscopy* 40, 86–90.
- Dargan, A.I., Khrapunov, S.N., Protas, A.F., Berdyshev, G.D., 1983. The change in maximum position of tyrosyl fluorescence spectra of R Nase A and histone dimer (H2A–H2B) under denaturation. *Stud. Biophys.* 96, 187–193.
- De Souza Sierra, M.M., Donard, O.F.X., Lamotte, M., Belin, C., Ewald, M., 1994. Fluorescence spectroscopy of coastal and marine waters. *Mar. Chem.* 47, 127–144.
- Determann, S., Reuter, R., Wagner, P., Willkomm, R., 1994. Fluorescent matter in the eastern Atlantic Ocean: Part 1. method of measurement and near-surface distribution. *Deep-Sea Res.* 41, 659–675.
- Determann, S., 1996. Analyse biologischer und biochemischer Prozesse im Meer mit Fluoreszenzspektroskopie. Ph.D. Thesis, University of Oldenburg, Germany, Shaker Verlag, Aachen, 1995, 168 pp.
- Determann, S., Reuter, R., Willkomm, R., 1996. Fluorescent matter in the eastern Atlantic Ocean: Part 2. vertical profiles and relation to water masses. *Deep-Sea Res.* 43, 345–360.
- Eisinger, J., Navon, G., 1969. Fluorescence quenching and isotope effect of tryptophan. *J. Chem. Phys.* 50, 2069–2077.
- Ewald, M., Stabel, H.-H., Belin, C., 1986. Composés organiques d'origine biogénique en Antarctique étudiés directement par spectrofluorimétrie. *Contes Rendues de l'Académie des Sciences Paris* 302, 883–886.
- Galla, H.J., Warnke, M., Scheit, K.H., 1985. Incorporation of the antimicrobial protein seminalplasmin into lipid bilayer membranes. *Eur. Biophys. J.* 12, 211.
- Guillard, R.R., Ryther, J.H., 1962. Studies of marine planktonic diatoms: I. *Cyclotella nana* Hustedt and *Detonula confervacea* (Cleve). *Gran Can. J. Microbiol.* 8, 229–239.
- Hansen, U.K., 1990. Structure and ligand binding properties of human serum albumin. *Dan. Med. Bull.* 37, 57–84.
- Hobbie, J.E., Daley, R.J., Jasper, S., 1977. Use of Nuclepore filters for counting bacteria by fluorescence spectroscopy. *Appl. Environ. Microbiol.* 33, 1225–1228.
- Kalle, K., 1963. Über das Verhalten und die Herkunft der in den Gewässern und in der Atmosphäre vorhandenen himmelblauen Fluoreszenz. *Deutsche Hydrographische Zeitschrift* 16, 153–166.
- Krause, G.H., Weis, E., 1991. Chlorophyll fluorescence and photosynthesis: the basics. *Annu. Rev. Plant Physiol. Plant Mol. Biol.* 42, 313–349.
- Lakowicz, J.R., 1986. Principles of fluorescence spectroscopy. Plenum, New York, 496 pp.
- Li, J.-K., Humphrey, A.E., 1990. Use of fluorometry for monitoring and control of a bioreactor. *Biotechnol. Bioeng.* 37, 1043–1049.
- Matthews, B.J.H., Jones, A.C., Theodorou, N.K., Tudhope, A.W., 1996. Excitation–emission-matrix fluorescence spectroscopy applied to humic acid bands in coral reefs. *Mar. Chem.* 55, 317–332.
- May, K.R., 1965. A new graticule for particle counting and sizing. *J. Scientific Instr.* 42, 500–501.
- Mopper, K., Schultz, C.A., 1993. Fluorescence as a possible tool for studying the nature and water column distribution of DOC components. *Mar. Chem.* 41, 229–238.
- Peters, T., 1985. Serum albumin. In: Anfinsen, C.B., Edsall, J.T., Richards, F.M. (Eds.), *Advances in Protein Chemistry*. Academic Press, Orlando, FL.

- Petersen, H.T., 1989. Determination of an *Isochrysis galbana* algal bloom by L-tryptophan fluorescence. *Mar. Pollut. Bull.* 20, 447–451.
- Reynolds, J.A., Tanford, C., 1970. The gross conformation of protein-sodium-dodecyl sulfate complexes. *J. Biol. Chem.* 245, 5161–5165.
- Robertson, K.J., Williams, P.M., Bada, J.L., 1987. Acid hydrolysis of dissolved combined amino acids in seawater: a precautionary note. *Limnol. Oceanogr.* 32, 996–997.
- Schneider, H.J., Földi, P., 1986. Amino acid analyses—a comparison of conventional and recent HPLC methods: Part II. *GIT Fachz. Lab.* 8, 873–889.
- Shelton, K.R., Rogers, K.S., 1971. Tryptophanyl fluorescence of sodium dodecyl sulfate treated and 2-mercaptoethanol reduced proteins: a simple assay for tryptophan. *Anal. Biochem.* 44, 134–142.
- Simon, M., Azam, F., 1989. Protein content and protein synthesis rates of planktonic marine bacteria. *Mar. Ecol. Prog. Ser.* 51, 201–213.
- Stryer, L., 1978. Fluorescence energy transfer as a spectroscopic ruler. *Annu. Rev. Biochem.* 47, 819.
- Tatischeff, I., Klein, R., 1976. Fluorescence quantum yield of the aromatic amino-acids as a function of excitation wavelength. In: Birks, J.B. (Ed.), *Excited states of biological molecules*. Wiley, London, pp. 375–387.
- Toulme, J.J., Le Doan, T., Helene, C., 1984. Role of tryptophyl residues in the binding of gene 32 protein from phage T4 to single-stranded DNA. Photochemical modification of tryptophan by trichlorethanol. *Biochemistry* 23, 1195–1201.
- Traganza, E.D., 1969. Fluorescence excitation and emission spectra of dissolved organic matter in sea water. *Bull. Mar. Sci.* 19, 897–904.
- Utermöhl, H., 1958. Zur Vervollkommnung der quantitativen Phytoplankton-Methodik. *Int. Ver. Theor. Angew. Limnol. Mittlg.* 9, 1–38.
- Wehry, E.L., Rogers, L.B., 1966. Fluorescence and phosphorescence of organic molecules: II. Photoluminescence and the structure of organic molecules. In: Hercules, D.M. (Ed.), *Fluorescence and phosphorescence analysis, principles and applications*. Wiley-Interscience, New York, pp. 81–99.
- Wehry, E.L., 1973. Effects of molecular structure and molecular environment on fluorescence. In: Guibault, G.G. (Ed.), *Practical fluorescence-theory, methods and techniques*. Decker, New York, pp. 79–136.
- Wolfbeis, O.S., 1985. The fluorescence of organic natural products. In: Schulman, S.G. (Ed.), *Molecular luminescence spectroscopy, methods and applications*, Vol. 77: Part I. Wiley-Interscience, New York, pp. 167–370.
- Zobell, E., 1946. *Mar. Microbiol.* Waltham, MA, 240 pp.